Biomedicine & Pharmacotherapy 131 (2020) 110671

Contents lists available at ScienceDirect

Biomedicine & Pharmacotherapy

journal homepage: www.elsevier.com/locate/biopha

Non-invasive bioassay of Cytokeratin Fragment 21.1 (Cyfra 21.1) protein in human saliva samples using immunoreaction method: An efficient platform for early-stage diagnosis of oral cancer based on biomedicine

Mohsen Jafari [a], Mohammad Hasanzadeh [b,*]

[a] Drag Applied Research Center, Tabriz University of Medical Sciences, Tabriz, Iran
[b] Pharmaceutical Analysis Research Center, Tabriz University of Medical Sciences, Tabriz, Iran

ARTICLE INFO

Keywords:
Oral cancer
Immunoassay
Cyfra 21.1
Biomedicine
Human saliva
Biotechnology

ABSTRACT

Oral cancer (OC) is considered as sixth most common cancer in the world. The challenge facing oral cancer is the lack of non-invasive, rapid, sensitive, accurate, and inexpensive screening and diagnosis methods. Given the increasing importance of prevention, prognosis, and early-stage diagnosis of cancer in improving of survival rate, the use of efficient diagnostic devices is essential. In this study, novel bioassay based on antigen and antibody immunocomplex was proposed for early stage diagnosis of OC. For the first time, an efficient immunosensor (CysGA-anti-Cyfra21.1-BSA-Cyfra21.1 antigen/AuE) was successfully designed and developed to the detection and determination of the Cyfra21.1 biomarker in unprocessed human saliva samples. The Au electrode was modified by Cysteamine (CysA) and Glutaraldehyde (GA) respectively via self-assembly as a substrate to immobilize the biological agents. The engineered immunosensor exhibit an excellent ability to detect and determine of Cyfra21.1 biomarker in low concentrations in unprocessed human saliva samples. Under the optimized operating conditions, the results demonstrate that the desired platform has a good sensitivity in the detecting of Cyfra21.1 with the low limit of quantitation (LLOQ) of 2.5 ng/mL, which this evaluation was performed at a wide linear range of 2.5−50 ng/mL. The use of the CysA-GA nano-hybrid as extraordinary stable substrate and extensive platform to place recognition elements was investigated using various electrochemical methods including cyclic voltammetry (CV) and square wave voltammetry (SWV). In this study, the engineered biosensor was used to non-invasive detection of Cyfra21.1 in unprocessed human saliva sample. Based on results, CysA-GA-anti-Cyfra21.1 antibody-BSA- Cyfra21.1 antigen/AuE with significantly high current intensity can provide appropriate, reliable, affordable, quick, and user-friendly diagnostic device to monitoring oral abnormality by detection and determination of Cyfra21.1 biomarker in human real sample. Above all, the easy to prepared designed immunosensor can be an extremely promising candidate to specific and favorable for a vast range of clinical diagnosis of OC in near future.

1. Introduction

Oral cancer (OC) is considered as sixth most common cancer in the world [1,2] and anatomically involves all malignancies in the lips, oral cavity, pharynx, and nasopharynx [3]. Oral squamous cell carcinoma (OSCC) is the most common and severe type of the disease [4] and generally occurs in the lateral edge of the tongue, the mouth floor, buccal mucosa and gingiva [4–6]. Furthermore this type of cancer accounts for 90 % of OC diagnostic cases [3]. Based on GLOBOCAN worldwide statistics on OC in 2012, estimated that OC accounted for 529,500 incident cases and 292,300 deaths, which is dedicated the 3.8 % of all cancer incidences, and 3.6 % of cancer deaths to itself. Also, the rate of incidence in men (4%) is two times more than women (2%), which can be related to more high-risk habits among men [7,8]. Geographical distribution is very various for the incidence of oral cancer worldwide, and the regions with the highest rates of incidences are in South and Southeast Asia. Sri Lanka, Bangladesh, Pakistan, and India are known as the countries with the highest rates of oral cancer for men, which 25 % of all cancer cases in these countries diagnosis as OC [9]. Due to the aging population and their exposure to many risk factors, it is estimated that the number of OC patients will reach 856,000 by 2035 [8].

* Corresponding author.
E-mail address: hasanzadehm@tbzmed.ac.ir (M. Hasanzadeh).

https://doi.org/10.1016/j.biopha.2020.110671
Received 10 July 2020; Received in revised form 17 August 2020; Accepted 20 August 2020
Available online 24 August 2020

Many of the risk factors involved in oral cancer considering the geographical distribution of the prevalence of oral cancer show that in developed countries, smoking and high alcohol consumption are determined as the causes of 75 % OC [10]. In developing countries, in addition to tobacco smoking, chewing areca-nut and Betel quid with or without tobacco are considered the most serious risk factor [11,12]. Consumption of high nitrosamines foods (e.g. salted fish) is also considered as a high-risk diet in increasing the risk of OC [11]. Infections caused by the high-risk human papillomavirus (HR-HPV) such as HPV-16 and HPV-18, as well as the Epstein-Barr virus (EBV) are increasingly becoming a serious risk factor for the prevalence of OC [13–15].

Determining the stage of OC is important because if malignancy is detected in stage T1, the survival rate is 90 %, while in stages T3 and T4 it drops to 20 % [16]. At a high-grade (T4), OC enters the metastatic stage and spreads to other organs of the body, mostly through the lymphatic system [17]. During metastasis of OC, cancer cells are able to move through the lymph to other organs in the body. The first and main organ to be targeted for OC metastasis are the lymph nodes in the neck [18]. The lung is also another target organ that significantly hosts oral cancer immigrant cells [18]. Therefore, early detection or prevention of the disease through screening of populations with a high risk of pre-cancerous lesions will be an effective strategy to prevent further outbreaks and control disease in initial grade (T1) or improve the treatment efficiency of oral cancer [19–21].

The challenge facing OC is the lack of non-invasive, rapid, sensitive, accurate, and inexpensive screening and diagnosis method [22]. Several methods for early diagnosis of OC neoplasia, includes: Toluidine blue staining, oral cytology/brush biopsy, Fluorescence spectroscopy, and imaging, chemiluminescent illumination, biopsy [23,24]. According to several reports, OC diagnostic assessments might take up to 6 months [25]. The current reliable method for diagnosing oral cancer is oral tissue biopsy with histopathological assessments of the tissue sample [26]. All of the above methods are generally expensive, invasive for the patient, time-consuming, require specialized equipment and technicians, the samples being assessments including blood, serum and tissue need to pretreatments [27]. Therefore, with the prevalence of cancers, extensive research is needed to find novel, detectable, high specificity, and sensitivity biomarkers with cost-effective and non-invasive methods [28,29].

Biomarkers are measurable indicators with the chemical nature of DNA, RNA, and protein that provide useful information about the state of health or disease of the body [30]. These compounds are present and can be measured in a variety of body fluids, such as saliva, blood, serum, and plasma, or in tissue samples taken from the different organs of the body [31].

Analysis and assessment of salivary biomarkers can be a proper, non-invasive, safe, inexpensive preparation alternative, and potential tools for clinical diagnosis of OC [31,32].

Whole of saliva is the result of the secretion of three main salivary glands, including sublingual, parotid glands, submandibular glands, and numerous small salivary glands. Saliva contains other compounds such as sputum, nasal secretions, blood from wounds or bleeding in the mouth, epithelial cells, food debris, and also there are microorganisms such as bacteria, viruses, fungi [33,34].

Biochemically, saliva is a transparent substance with an average protein concentration of 1.5−2 mg/mL. Saliva has a high potential for early detection of diseases due to its wide range of biomolecules [35]. In recent years, many studies have been conducted on the diagnosis of lung, breast, oral, and pancreatic cancer which demonstrate the saliva reliability for wide range of disease diagnoses application [36]. In addition, blood and serum samples are much more complex than saliva due to a wide range of macromolecules, and interference from their macromolecules can lead to errors in an accurate diagnosis [37]. Complete saliva is one of the most reliable and accurate tools for diagnosing OC in early stage due to its direct contact with the oral cavity [36,38]. Nowadays researchers have identified more than 100 potential salivary biomarkers [31].

Cytokeratin family (CKs) contains 19 different peptides (CK-1 to CK-19), which are classified into two subtypes: type I (Acidic type, molecular weight: 40−56 kDa) and type II (Basic type, molecular weight: 53−67 kDa). Cytokeratin-19 is an acidic subunit of type I that is present in all simple squamous cells and in cancers arising from them [36,39]. Cyfra 21.1 is a soluble fragment of cytokeratin-19 that is released during cell apoptosis. Cyfra 21.1 is also found as a potential biomarker in many epithelial cell cancers [27]. The utilization of Cyfra 21.1 as a biomarker of OC was first proven by Kurokawa and coworkers [36]. The Cyfra 21.1 antigen is secreted in large amounts in saliva. In normal individuals, levels of Cyfra 21.1 have measured 3.8 ng/mL while in cancer patients, it is increased to 17.46 ± 1.46 ng/mL [36]. Various clinical studies have shown that Cyfra 21.1 salivary biomarkers are approved and reliable for early detection of OC [40–43].

Immunosensors are a branch of biosensors whose mechanism of action is based on identifying the binding of the antigen to its specific antibody and the formation of a stable and irreversible antibody-antigen complex [44,45]. Immunosensors are attractive and useful instruments for diagnostic applications because the binding of the antigen to its specific antibody significantly increases the specificity of the diagnostic measurement and makes it possible to accurately detection and determine the value of biomarkers in the most complex biological samples [46,47]. Therefore, all types of electrochemical biosensors, especially electrochemical immunosensors have attracted a lot of attention in medical diagnosis purposes, due to their inexpensive, user-friendliness, simple equipment and ease of use, real-time measurement, high sensitivity and specificity, portability, and proper performance with low sample values [27,48–50].

One of the most important components in the preparation of an electrochemical (EC) immunoassay is a highly reactive, electroactive, and stable substrate to immobilize the immunological elements at its surface and improving the electrical conductivity for effective assessment [51]. For this purpose, substrates made nanomaterials play an important role. Substrates modified of nanomaterial via different methods create an extensive range of features, such as increased surface area, which allows lots of protein to be immobilized at the electrode substrate surface [52,53]. In addition to its significant electrical properties, the use of nanomaterials also plays a key role in improving the stability and sensitivity of the EC biosensors [54].

Cysteamine (CysA) is an outstanding nanomaterial used to modify the electrode surface of electrochemical biosensors by having high-performance functional groups in establishing covalent bonding [55]. The thiol group in the cysteamine structure has been identified as an accelerator of electron transfer in redox reactions of the electrode surface and mediator solution [55]. Au and CysA form strong bonds by establishing a covalent bond between thiol groups. Also, with the completion of the interaction, cysteamine's free amine groups are provided for interaction with antibodies carboxyl groups to immobilize it at the electrode surface by establishing a covalent bond, which is playing the important role in the stability of the desired immunosensors [51].

Self-assembly monolayers (SAM) can be considered as one of the most efficient and popular strategies for the preparation of novel substrate modified by advanced nanomaterials towards biosensing [56]. SAM refers to the process of organizing and spontaneously assembling of adsorbate materials at different substrates [57]. SAM occurs in the initial step as physical absorption through direct contact with the substrate. In the second step, the tendency of chemical adsorption between the adsorbent and the substrate due to the interaction of reactive chemical groups and the formation of strong chemical bonds leads to the formation of a stable monolayer substrate [58]. Using the SAM method to modify the gold electrode surface by thiol groups due to having a disulfide reactive group is one of the most efficient and desirable methods of preparing the substrate with favorable and stable electrochemical properties [59]. The other favorable features obtained in the use of SAM

are: simplicity and need to a little volume of nanomaterials, easy organization, creating an appropriate surface area for immobilizing the biomolecules, improving the sensitivity with a significantly reduce double-layer charge current, and reproducibility [56,60].

Briefly, the electrochemical properties of CysA modified nanomaterials have encouraged us to investigate the possibility of providing a platform based on CysA-GA to immobilize the anti-Cyfra21.1antibody (Ab) to identify Cyfra 21.1 biomarker in the purpose of early detection of oral cancer. The CysA-GA nanocomposite substrate increases the accessible contact area to immobilization of antibody, thus they could increase the active surface to interact with Cyfra 21.1 which can lead to enhance sensitivity of electrochemical assessment. This process also represents and confirms the increase in the geometric surface, which is very important parameter in electrochemistry. The excellent chemical properties of the CysA-GA substrate due to its thiol groups and strong interaction with the Au electrode on the one hand, and subsequently the free amine end for interaction with the antibody, has received more attention for preparation of high efficiency modified electrode. Step-by-step preparation of CysA-GA-anti- Cyfra21.1 Ab-BSA-Cyfra21.1 antigen/AuE immunosensor in the biological and non-biological section was monitored by the cyclic voltammetry (CV) and the square wave voltammetry (SWV). Also, the redox behavior of the prepared immunosensor at each stage was characterized by the mentioned techniques. Furthermore, the engineered immunosensor was investigated to detection and determination of the Cyfra 21.1 biomarker in real samples. The investigation of the designed immunosensor was performed on both the standard antigen sample and the real human saliva sample by CV and SWV, and the results show that the engineered immunosensor is a novel platform for detection of Cyfra 21.1 biomarker in the human salivary sample with good sensitivity. As well as, the low limit of quantification was measured at 2.5 ng/mL. To the best of our knowledge, this is the first time that the CysA-GA interface has been used as a substrate for anti- Cyfra 21.1 antibody immobilization to the detection of Cyfra 21.1 biomarkers with the aim of, noninvasive, inexpensive, easy, user-friendly and early detection of OC by using untreated and unstimulated human saliva samples.

2. Experimental

2.1. Materials and reagents

All chemicals used in this research are in analytical grade. Human Cytokeratin Fragment Antigen 21-1 (CYFRA21-1) ELISA Kit was purchased from MyBiosource (San Diego, California, USA). Sodium hydrogen phosphate (Na_2HPO_4), Sodium dihydrogen phosphate monohydrate ($H_2NaPO_4.H_2O$), Potassium ferrocyanide ($K_4Fe(CN)_6$), Potassium ferricyanide ($K_3Fe(CN)_6$), Potassium chloride (KCL) were bought from Merck (Germany). Cysteamine (CysA), Glutaraldehyde (GA), Bovine serum albumin (BSA) were purchased from Sigma Aldrich (Ontario, Canada). Ethanol and Sulfuric acid supplied from Scharlau Chemie S.A.

2.2. Solutions

To obtain the desired matrix, we first prepare a 10 mM solution of CysA using a 1 mM ethanol solvent. 1 mM of ethanol is also used for washing. Phosphate-buffered saline (PBS) solution was prepared at pH = 7.4 in a concentration of 0.1 M and used as washing and diluting Solution. Ferrocyanide/Ferricyanide $[Fe(CN)_6]^{-3/-4}$ solution containing KCl was also prepared as an electrochemical mediator solution at a concentration of 0.01 mM. The solution of H_2SO_4 (0.1 M) was prepared for cleaning the inorganic compound from the electrode surface before usage. Also, an acetone and water mixture solution in 1:1 ratio was used to remove of organic contaminants. GA as a cross-linking agent was used in standard grade. All solutions used in this work were prepared daily and fresh.

2.3. Human saliva sample collecting

An unprocessed salivary sample of a healthy volunteer was obtained in the following method.

Saliva sample collection was performed in the early hours of the morning. To ensure that the oral cavity is free of food debris or any non-biological material, the saliva donor was asked to do not eat food and avoid drinking any liquids and chewing gum for at least 8 h after the necessary cleansing at night (such as teeth brushing, use mouthwash liquid and etc.). Thus, the saliva sample was taken from the volunteer in the full fasting state.

In order to ensure that the oral cavity is completely clean before collecting the salivary sample, the final washing was performed before sampling in the oral cavity with PBS (0.1 M, pH = 7.4) for 30 s. Therefore, 5 mL of PBS solution was completely rotated in the oral cavity and then the solution was thrown away. Then, 2 mL of saliva sample was transferred to the microtube after 20 s after rinsing the mouth. The transparency of the obtained sample was examined and no additional suspended particles were observed in it.

2.4. Instruments

Electrochemical experiments for voltammetric measurements were accomplished in three-electrode cell (from Metrohm) powered by an electrochemical system consisting of PalmSens 4c system, electrochemical interface. The system was run on a laptop using PSTrace5 software. Electrochemical system was composed of conventional three-electrode cell was utilized with an Ag/AgCl (Methrom, The Netherlands) as a reference electrode, and a Pt wire was used as a counter-electrode. The working electrode was gold electrode (AuE) (d =2 mm) (from Azar electrode Co., Iran). The surface morphology of the modified electrodes was evaluated with a MIRA3 FEG-SEM (SEM, Hitachi Ltd., Czech,). Before modification, Au electrode was polished to a mirror-like finish with 0.3 and 0.05 mm alumina slurry (Beuhler, USA) followed by rinsing thoroughly with double distilled water.

2.5. Fabrication of immunosensor

Prior to modification, the electrodes are continuously polished with alumina, covered with a polishing cloth. It is then immersed in a solution of water and acetone (ratio 1:1) for 30 min and then it is placed in an electrochemical cell containing 0.1 M H_2SO_4 for electrochemical cleaning, and 20 cycles are applied to it at a potential range of -1.5 to 0 at a scan rate of 100 mV/s. Then, electrodes rinsed with deionized water and dried in room temperature. After complete cleaning, the electrode surface was modified by self-assembly method.

In purpose of electrodes modification by complete chemical self-assembly method as an efficient and affordable manner for sensing and biosensing applications, in the first step, the bare Au electrode was immersed in CysA solution (200 μL of 10 mM) for 3 h and stored in dark and room temperature conditions. After the prescribed time, CysA modified Au electrode (CysA/AuE) rinsed with 1 mM of ethanol and dry with N_2 gas. Immediately after that, CysA/Au electrode was immersed in the solution containing GA and put it at room temperature for 30 min to establish and improvement of cross-linkage between CysA and GA. In the next step, after removing the electrode from the GA solution, it was rinsed with a PBS solution (0.1 M, pH = 7.4) and then was dried with N_2 gas.

After preparation of CysA-GA/AuE, desired modified electrode was incubated in a 50 μl of anti-Cyfra 21.1 antibodies for 12 h at 4 °C. Then in purpose of blocking non-specific binding of anti-Cyfra 21.1 antibody, CysA-GA/ anti-Cyfra 21.1 antibody/AuE immersed in BSA solution for 1 h. Afterwards, Cyfra 21.1 antigen incubated on surface of CysA-GA-anti-Cyfra 21.1 antibody-BSA/AuE and placed in 4 °C for 5 h. The whole fabrication procedure of desired CysA-GA- anti-Cyfra 21.1 antibody-BSA-Cyfra 21.1 antigen/AuE immunosensor for Cyfra 21.1

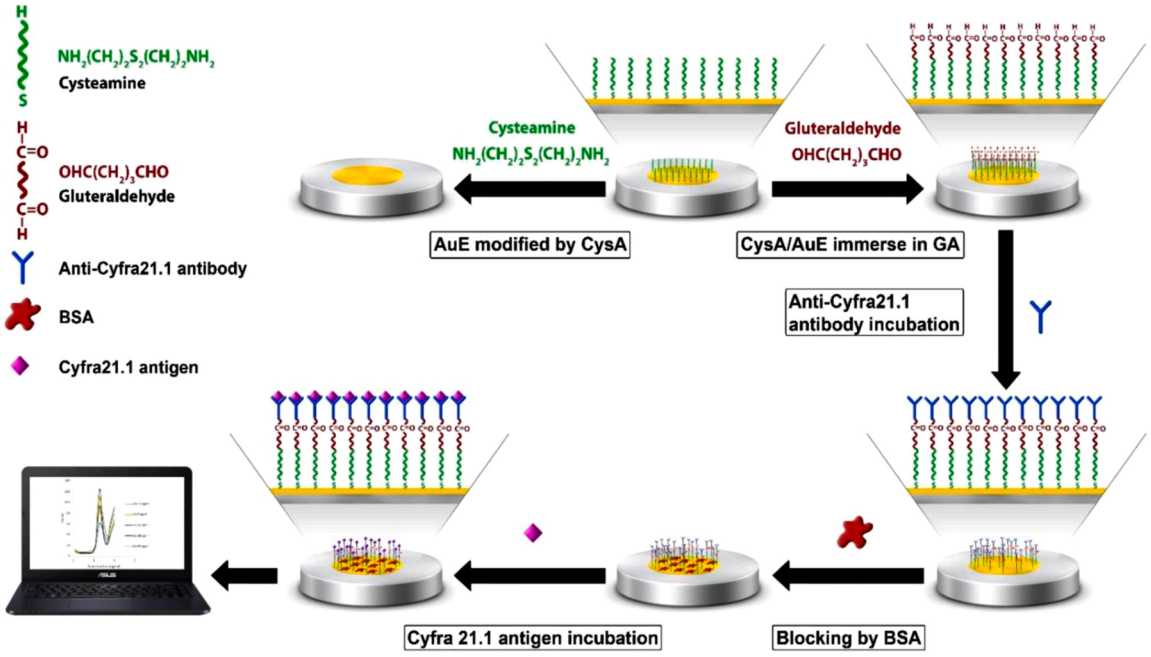

Scheme 1. The fabrication procedure of electrochemical immunosensor for Cyfra21.1 detection.

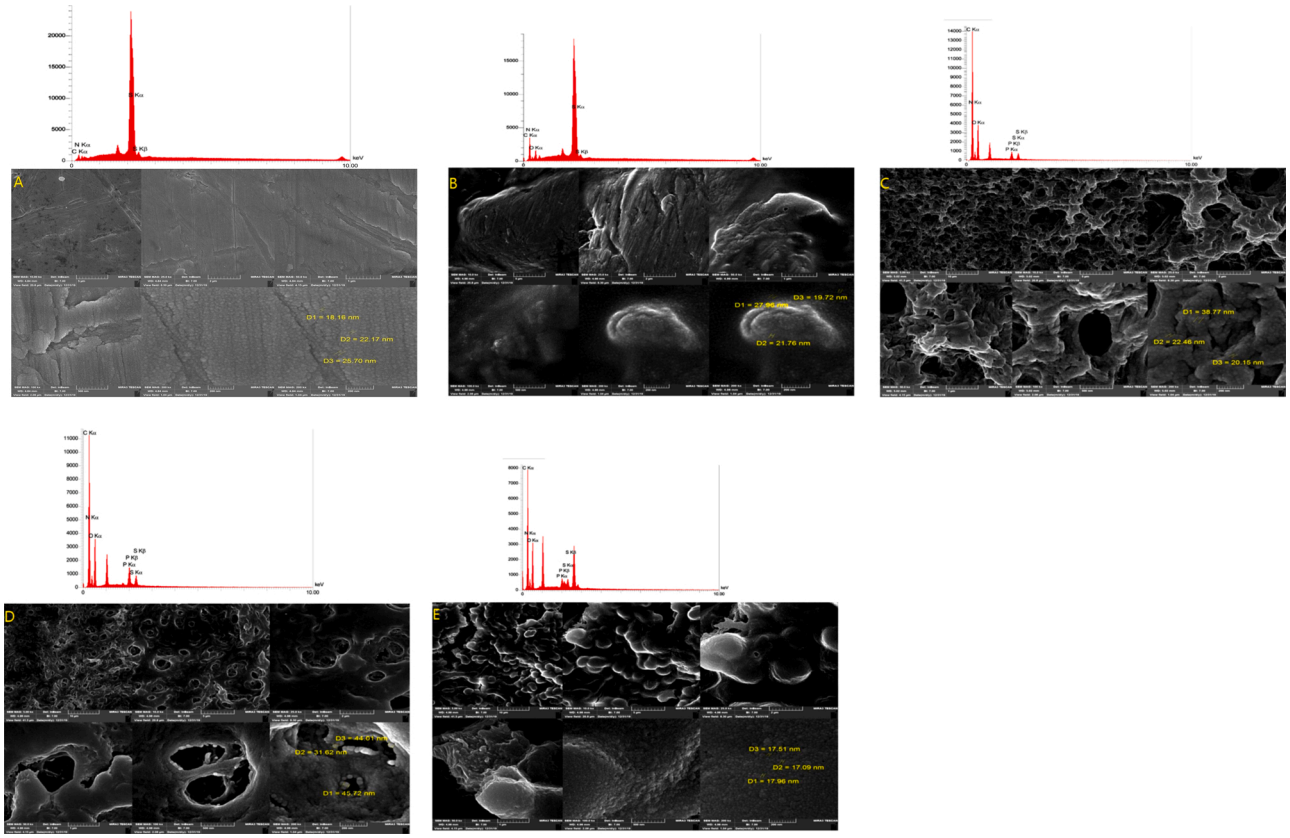

Fig. 1. A. FE-SEM images of CysA/AuE in different magnification and its related EDS result. B. FE-SEM images of CysA-GA/AuE in different magnification and its related EDS result. C. FE-SEM images of CysA-GA- anti-Cyfra21.1 antibodies/AuE in different magnification and its related EDS result. D. FE-SEM images of CysA-GA-anti-Cyfra21.1 antibodies-BSA/AuE in different magnification and its related EDS result. E. FE-SEM images of CysA-GA-anti-Cyfar21.1 Ab-BSA-Cyfra21.1 antigen/AuE in different magnification and its related EDS result.

detection was illustrated in Scheme 1. It should be noted that after all steps of biological incubation, the obtained electrodes was rinsed with PBS (0.1 M, pH = 7.4) solution.

2.6. Characterization of fabricated immunosensor

In following, the FE-SEM imaging obtained results for five modified

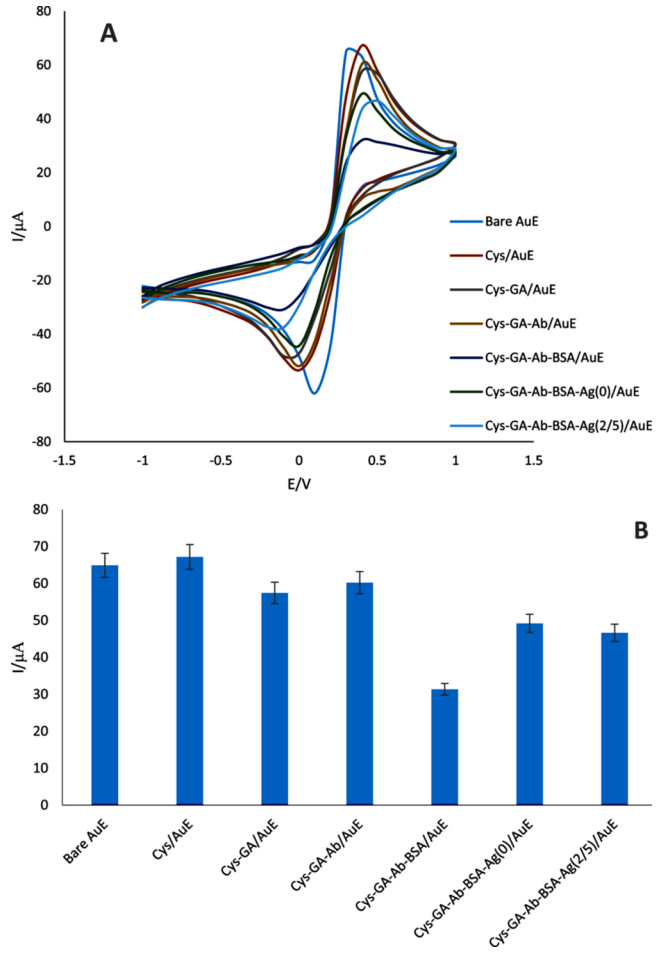

Fig. 2. CVs voltammogram (A) and oxidation peak's current histogram (B) in the potential range of -1 to +1 V for bare AuE, CysA/AuE, CysA-GA/AuE CysA-GA-anti-Cyfra21.1/AuE, CysA-GA-anti-Cyfra21.1-BSA/AuE, CysA-GA-anti-Cyfra21.1-BSA-Cyfar21.1 antigen/AuE. Supporting electrolyte is 0.01 M [Fe (CN) 6]3-/4- solution containing KCl.

Au electrode by CysA, CysA-GA, CysA-GA-anti Cyfra 21.1 antibody, CysA-GA-anti Cyfra 21.1 antibody-BSA, CysA-GA-anti Cyfra 21.1 antibody-BSA- Cyfra 21.1 antigen was shown in Fig. 1(A–E). As the images reveal, polymer films have grown by self-assembly on the surface of Au electrode. The formation of CysA shown in different magnification in Fig. 1A with an average diameter of 22.17 nm has been recorded. Also, EDS results confirmed the presents of S, N and C elements on surface of AuE. Furthermore, FE-SEM imaging in Fig. 1B was recorded after utilizing GA as a stabilizer agent with lowest detected diameter of 19.72 nm. As well as, EDS obtained results reveals that in addition to S, C and N as prepared matrix elements, oxygen also appeared at the matrix as one of the elements in the GA structure.

In subsequent, the stage of antibody incubation in different magnifications is shown in Fig. 1C. Compared to the previous stage (CysA-GA), the structures containing the pores in the image are observed, which indicates the success of the electrode modification process at this stage. Based on EDS curve, the results confirm the presence of elements C, O, N, S and P on the surface of AuE. The use of BSA blocking agent in electrode surface modification to block non-specific bonds is shown in Fig. 1D with different magnifications. By comparing the images of the blocking stage with the previous one, it is clear that the structures formed by anti-Cyfra 21.1 antibody incubation are significantly blocked. According to the EDS curve, the results confirm the presence of C, O, N, S, and P elements on the surface of AuE.

In the last step, the CysA-GA-anti-Cyfra 21.1 Ab-BSA- Cyfra 21.1 antigen/AuE was evaluated by FE-SEM and results are shown in Fig. 1E. Comparative observation of the images demonstrates that the Cyfra 21.1 antigen binds to its specific antibodies after the blocking stage with BSA. Based on the EDS curve, the results confirm the presence of C, O, N, S, and P elements on the surface of AuE.

3. Results and discussion

3.1. Electrochemical behavior of engineered immunosensor

The electrochemical behavior of bare Au electrode before and after modification with mentioned materials and biological elements were investigated by some voltammetric techniques including cyclic voltammetry (CV) and square wave voltammetry (SWV). According to the data obtained from the CV and SWV techniques for the evaluation of each step, electrode modification was performed in one complete cycle, in the potential range of -1 to +1 V and the sweep rate of 100 mV/s in the 0.01 M $[Fe(CN)_6]^{-3/-4}$ solution containing KCl.

According to Fig. 2A & B, CVs was performed to evaluate the electrochemical behavior of electrodes bare AuE, CysA/AuE, CysA-GA/AuE, CysA-GA-anti-Cyfra21.1/AuE, CysA-GA-anti- Cyfra21.1-BSA/AuE, CysA-GA-anti-Cyfra21.1-BSA- Cyfra21.1 antigen/AuE under the above-mentioned conditions, respectively. The results show that the bare Au electrode shows a peak current in 64.9 μA, which is related to intrinsic feature of gold as a conductive metal. In the next step, after modifying the electrode surface with CysA, peak current was reached to 67/1 μA and also a change in oxidation peak position is observed, which can confirm the successful modification of the AuE with CysA. Following the modifying process by GA, which is used as a stabilizer to establish cross-links, a decrease in current is observed.

The entrance into the immobilization step of biological agents begins with anti-Cyfra21.1 antibody incubation. After immobilization of the antibody at the matrix of surface, the CVs assessments show that the current intensity has increased. Antibodies were expected to further reduce current intensity by blocking the matrix surface, but an investigation of the antibody structure in FE-SEM images demonstrates that the nature of the porous structure of the anti-Cyfra21.1 antibody on the

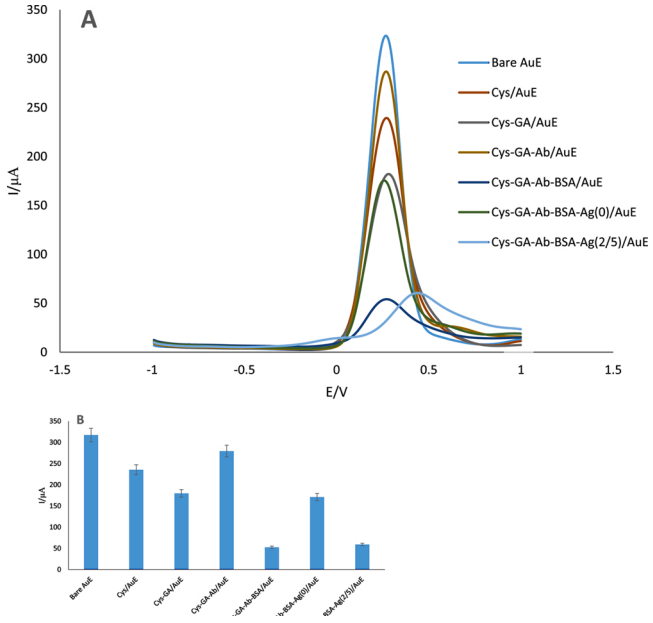

Fig. 3. SWVs voltammogram (A) and histogram (B) in the potential range of -1 to +1 V for bare AuE, CysA/AuE, CysA-GA/AuE CysA-GA-anti-Cyfra21.1/AuE, CysA-GA-anti-Cyfra21.1-BSA/AuE, CysA-GA-anti-Cyfra21.1-BSA-Cyfar21.1 antigen/AuE. Supporting electrolyte is 0.01 M [Fe (CN) 6]3-/4- solution containing KCl.

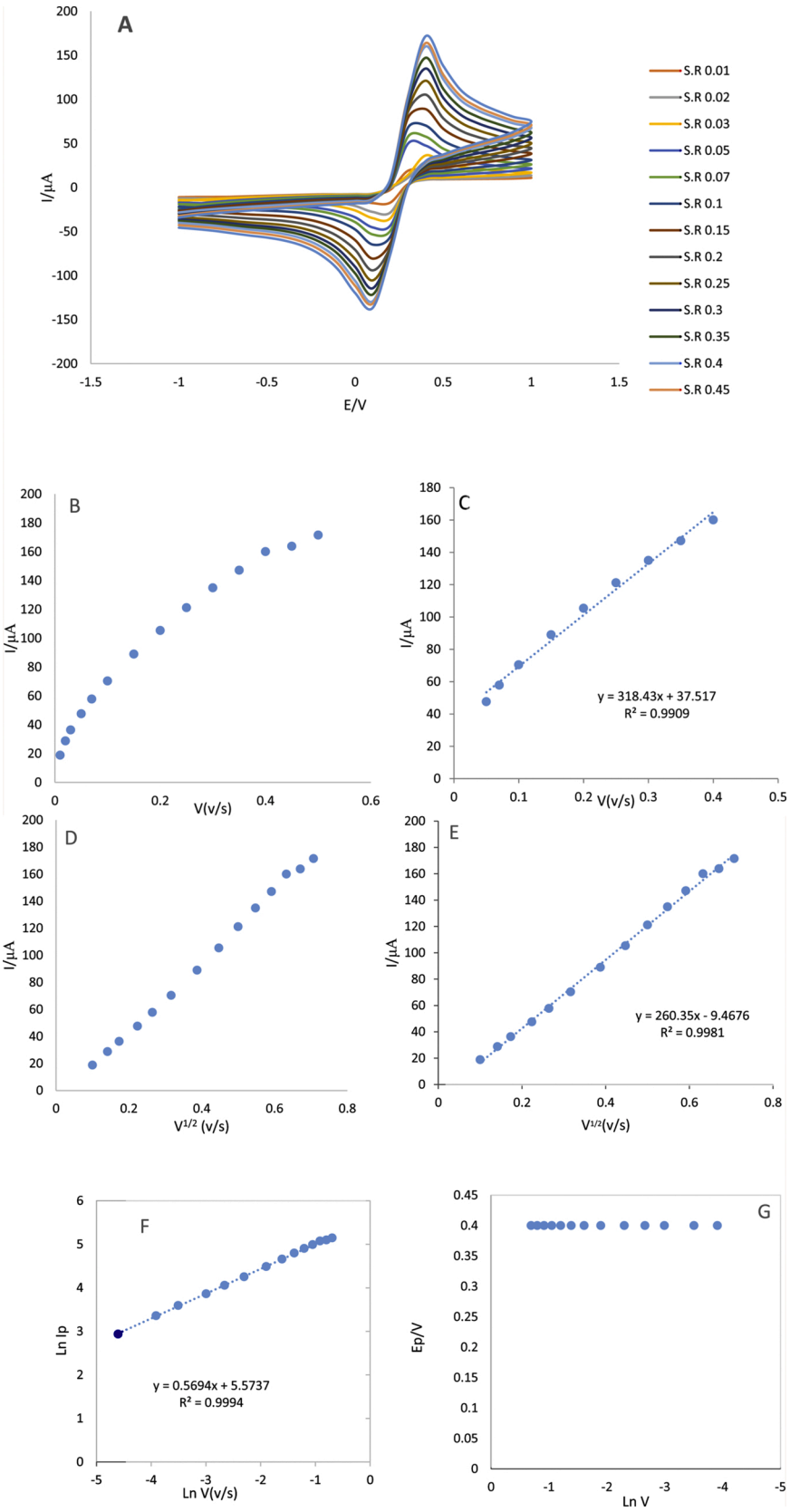

Fig. 4. A) CVs of CysA/AuE in potential range of -1 to +1 in different sweep rate of 10 to 500 mV/s in 0.01 M [Fe (CN) 6]3-/4- solution containing KCl. B) Variations of oxidation peak currents versus different sweep rate. C) calibration curve of oxidation peak current versus different sweep rate. D) Variations of oxidation peak currents versus square root of different sweep rate. E) calibration curve of oxidation peak currents versus square root of different sweep rate. F) Calibration curve of oxidation peak's current versus sweep rate in terms of Neperian logarithm. G) Variation of oxidation peak potential versus Neperian logarithm of sweep rate.

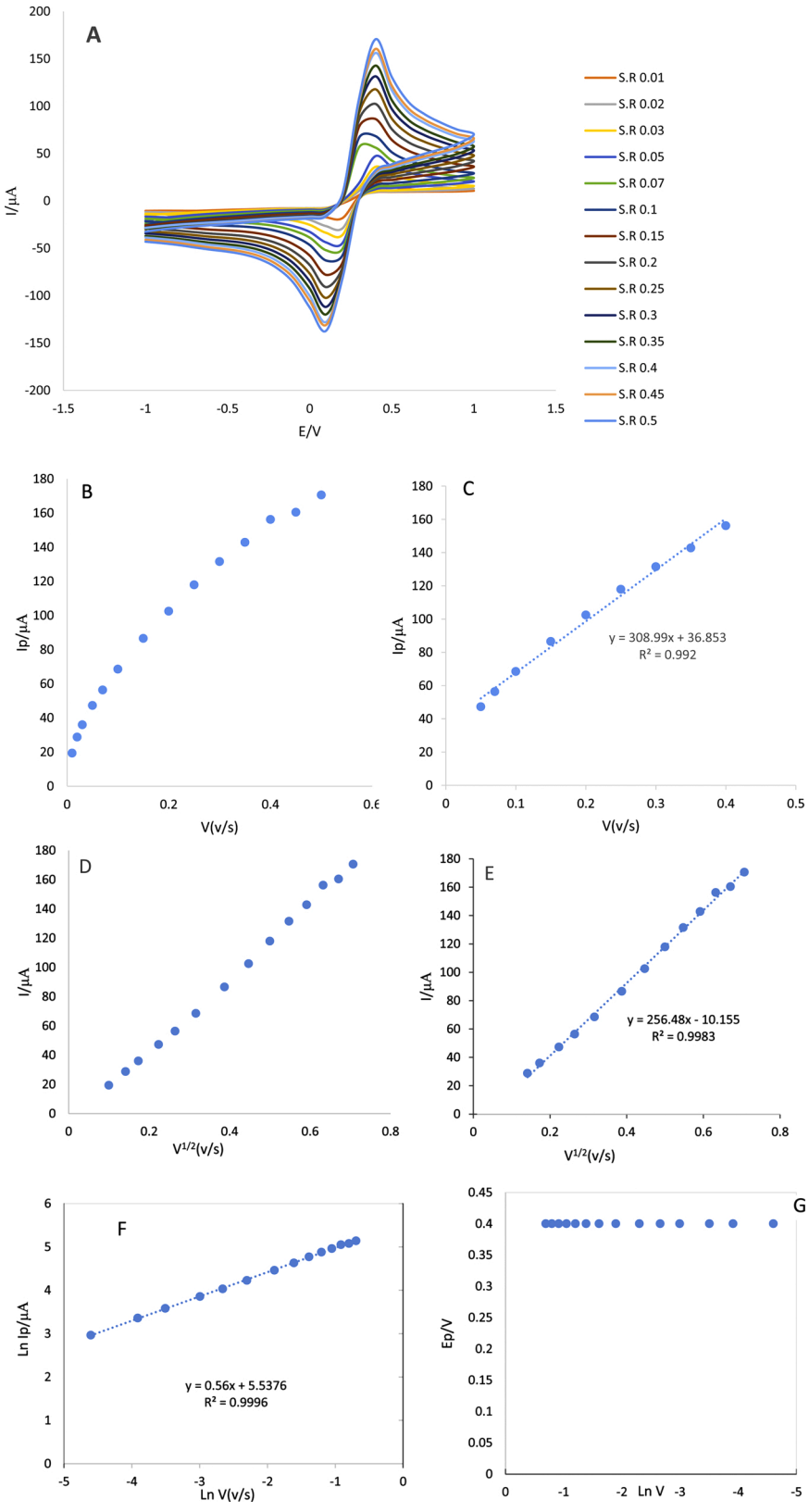

Fig. 5. A) CVs of Cys/AuE in potential range of -1 to +1 in different sweep rate of 10 to 500 mV/s in 0.01 M [Fe (CN) 6]3-/4- solution containing KCl. B) Variations of oxidation peak currents versus different sweep rate. C) calibration curve of oxidation peak current versus different sweep rate. D) Variations of oxidation peak currents versus square root of different sweep rate. E) calibration curve of oxidation peak currents versus square root of different sweep rate. F) Calibration curve of oxidation peak's current versus sweep rate in terms of Neperian logarithm. G) Variation of oxidation peak potential versus Neperian logarithm of sweep rate.

CysA-GA modified electrode surface and its interaction with the matrix has accelerated the flow of electrons at the electrode surface. Therefore, oxidation peak current indicates a higher current density than CysA-GA. Considering the increase in current intensity in the antibody incubation step, it can be concluded that the use of BSA by blocking the surface should reduce the current intensity, and in the following, CVs assessment confirms the electrochemical behavior of electrode modified with BSA that CysA-GA-anti-Cyfra21.1 antibody-BSA/AuE indicates the lowest current intensity (31 µA).

The last step in completing the immunosensor construction is adding

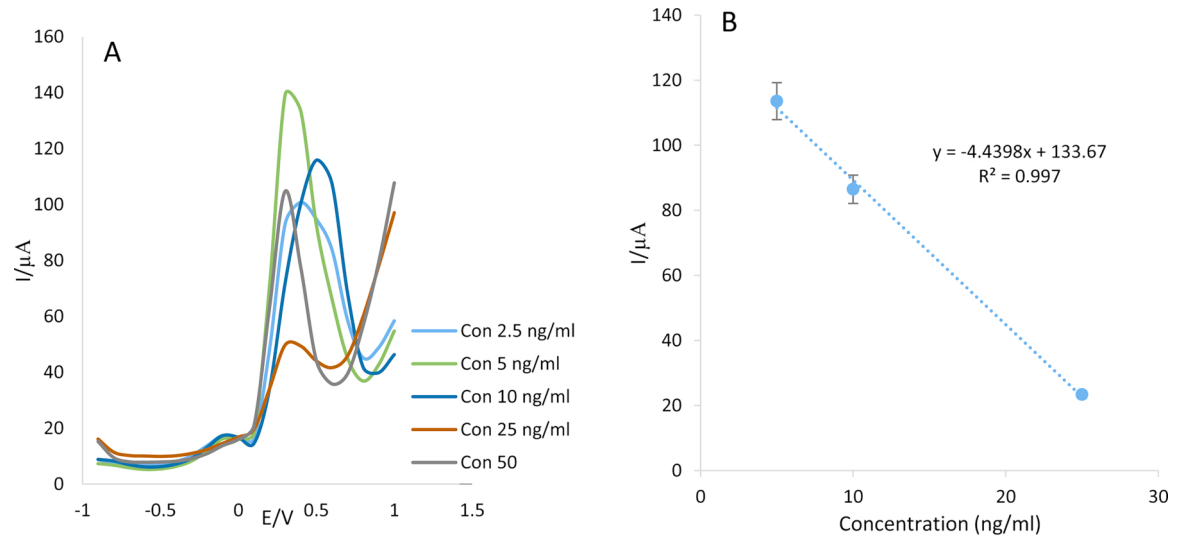

Fig. 6. A) SWVs responses of the immunosensor for different concentrations of Cyfra21.1: 2.5, 5, 10, 25, 50 ng/mL in 0.01 M [Fe (CN) 6]3-/4- solution containing KCl. B) Calibration curve (n = 5, Sd = 1.39, Sd = 1.33, Sd = 1.30 for concentrations of 5, 10, and 25 ng/mL, respectively).

the Cyfra21.1 antigen to the CysA-GA-anti-Cyfra21.1 antibody-BSA/AuE complex and investigating the interaction of the antigen with the specific antibody. For this purpose, two concentrations of antigens were evaluated to assess the accuracy of the designed immunosensor. Standard concentration of Cyfra21.1 antigen incubation was associated with a change in peak current intensity. Another electrode was prepared and evaluated for 2.5 ng/mL standard concentration of Cyfra21.1 antigen, and the results showed that increasing the antigen concentration was reduce the current intensity by limiting electron transfer at the surface of the designed immunosensor.

For further evaluation of the electrochemical behavior of the designed immunosensor, SWV was recorded step by step (Fig. 3A & B) and the results confirm the recorded electrochemical behavior of the designed immunosensor by the CV.

3.2. Kinetic study

Scan rate is used as an effective index in the investigation of redox reactions for various compounds, also useful information including electrochemical mechanisms of electron transfer can be obtained from the association between the peak's current and potential to sweep rate. Therefore, the typical CVs were performed at potential range of -1 to +1 V and various scan rate from 10 to 500 $mV.s^{-1}$ to kinetic study of engineered interface of CysA/AuE in 0.01 M $[Fe(CN)_6]^{-3/-4}$ solutions (Fig. 4A) and obtained related plot was shown in Fig. 4B. Furthermore, the plot of oxidation linear peak currents to sweep rate shown in Fig. 4C, pointing to electrochemical activity of surface redox couple.

$$Ip = \left(\frac{n^2 F^2}{4RT}\right)\nu A\Gamma* \quad (1)$$

Where $\Gamma*$ is the surface coverage of the redox species, ν being the potential sweep rate and A is the electrode surface area ($A = \pi r^2 = 0.0314$ cm^2). $\Gamma*$ has been obtained as 106.5×10^{-9} mol. cm^{-2}. Based on the peak currents versus sweep rate squared obtained result shown in Fig. 4E which linear slope related to it, reliable to demonstrate a mass transfer controlling process of oxidation occurred via diffusion. To characterize the type of couple reaction system the CV recorded has certain well-defined characteristics, including investigation of the peaks potential position and peaks height changes in proportional to scan rate increasing. According to the voltammogram recorded for CysA/AuE, it can be concluded that the type of coupled reaction system is reversible because the positions of peak potential do not alter as a function of scan rates alteration. Then, it can be stated that it is the reversible diffusion-controlled process.

In the case of CysA-GA/AuE kinetic study, typical CVs were performed at the potential range of -1 to +1 V in the various scan rates from 10 to 500 $mV.s^{-1}$ in 0.01 M $[Fe(CN)_6]^{3-/4-}$ solutions (Fig. 5A) and related curve for obtained results were shown in Fig. 5B. Furthermore, dependency of oxidation linear peak currents to sweep rate shown in Fig. 5C, pointing to the electrochemical activity of the surface redox couple, which was obtained by using line slope of Eq. (1). According to the calculations performed with Eq. (1), $\Gamma*$ has been obtained 104.72×10^{-9} mol. cm^{-2}. Due to the variation peak currents *versus* sweep rate squared obtained result shown in Fig. 5E which linear slope related to it, reliable to demonstrate a mass transfer controlling process of oxidation occurred via diffusion.

For CysA-GA/AuE engineered matrix, the couple reaction system was studied via investigation of the peaks potential and peaks height changes in proportional to scan rate. According to the voltammogram recorded for CysA-GA/AuE, it can be concluded that the type of coupled reaction system is reversible because the positions of peak potential do not alter as a function of scan rate. Then, it can be stated that it is the reversible diffusion-controlled process.

As can be deduced from the calculation of the surface coverage of the redox species for the CysA/AuE and CysA-GA/AuE matrix, after incubation of the CysA/Au modified electrode with GA, the surface coverage reduced, as the cross-links resulting from the interaction of GA with CysA that increases the stability of the substrate.

3.3. Analytical performance

3.3.1. Sensitivity study in standard samples

The CysA-GA-anti-Cyfra21.1 antibody -BSA-Cyfra21.1-antigen/AuE immunosensor analytical performance was investigated by SWVs techniques in different concentrations of Cyfra21.1 biomarker. SWVs was recorded at different concentrations of Cyfra21.1 biomarker (2.5, 5, 10, 25, 50 ng/mL) in a standard sample with a sweep rate of 100 mV / s in the potential range of -1 to +1 V and the results were shown in Fig. 6A. According to Fig. 6B, the calibration curve of immunosensor at various concentrations of Cyfra21.1 was plotted by SWV which shows the linear regressions equation for concentrations ranging from 2.5 ng/mL to 50 ng/mL and confirm the engineered immunosensor ability to sensitive analysis of biomarker using SWV technique. The obtained linear regressions equation is as follows:

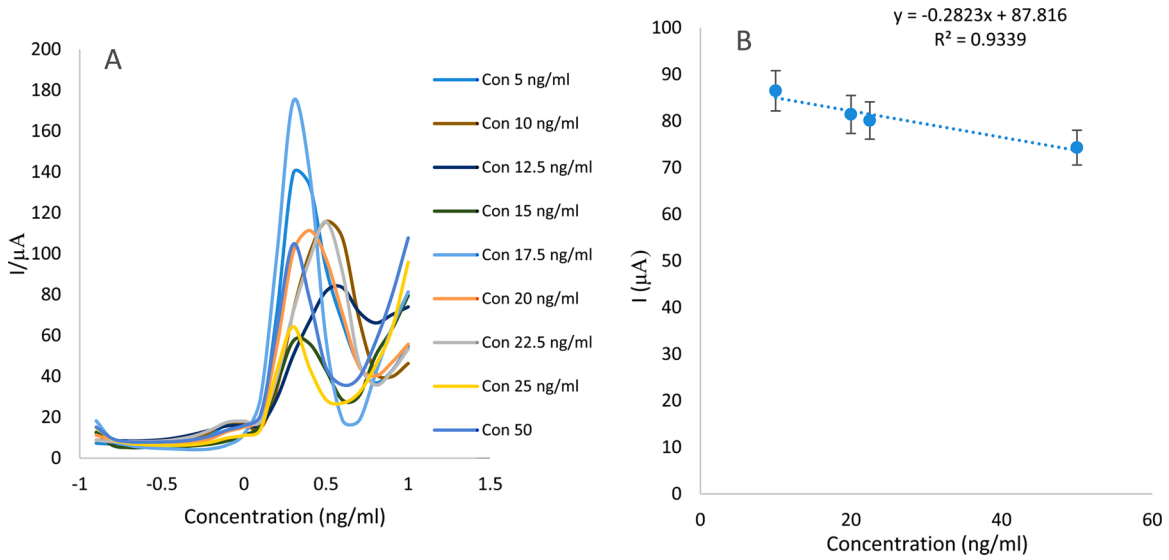

Fig. 7. A) SWVs responses of the immunosensor for different diluted concentrations of Cyfra21.1: 5, 10, 12.5, 15, 17.5, 20, 22.5, 25, 50 ng/mL in 0.01 M [Fe (CN) 6] 3-/4- solution containing KCl. B) Calibration curve (n = 5, Sd = 2.52, Sd = 2.54, Sd = 2.53, and Sd = 2.57, for concentrations of 10, 20, 25, and 50 ng/mL, respectively).

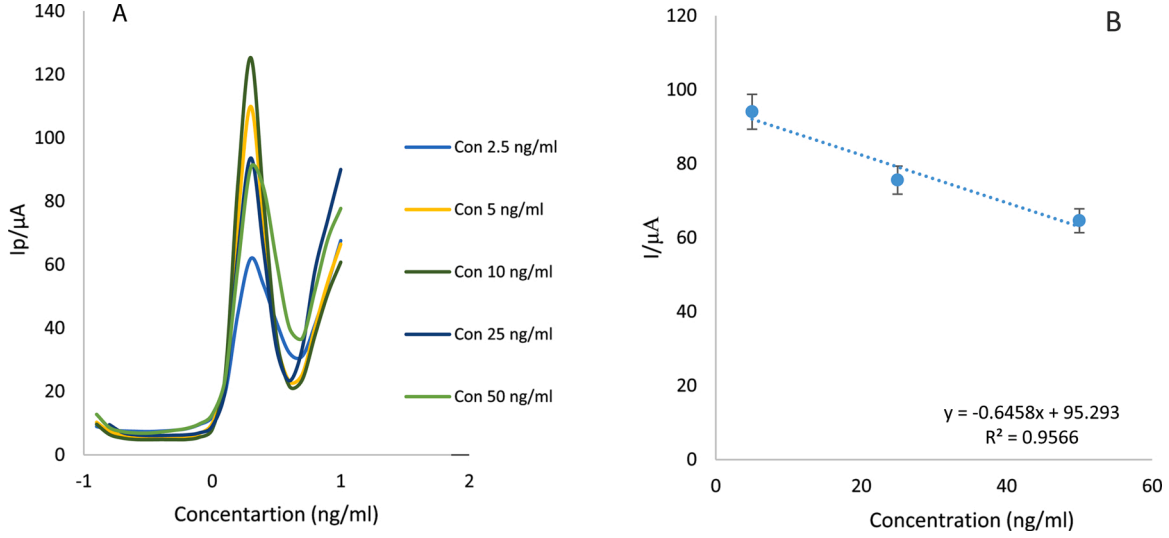

Fig. 8. A) SWVs responses of the immunosensor for different concentrations of Cyfra21.1: 2.5, 5, 10, 25, 50 ng/mL in human saliva sample in 0.01 M [Fe (CN) 6]3-/4- solution containing KCl. B) Calibration curve (n = 5, Sd = 2.23, Sd = 2.21, and Sd = 2.20, for concentrations of 5, 25, and 50 ng/mL, respectively)).

$I\ (\mu A) = -4.4398\ C_{(CYFAR21.1)} + 133.67,\ R^2 = 0.997.$

In order to evaluate the desired immunosensor, different concentrations of Cyfra21.1 antigen between 10 ng/mL to 25 ng/mL was prepared. Prepared diluted concentrations were 12.5, 15, 17.5, 20, 22.5 ng/mL respectively. According to Fig. 7, the evaluation of immunosensor sensitivity was performed in the range of 5 ng/mL to 50 ng/mL by mentioned diluting concentrations using SWV technique.

The linear regressions equation in the concentration range of 5−50 ng/mL was obtained as:

$I\ (\mu A) = -0.2823\ C_{(Cyfra21.1)} + 87.816,\ R^2 = 0.9339.$

The lower limit of quantification (LLOQ) for the detection of the Cyfra21.1 antigen as candidate biomarker was obtained as 2.5 ng /mL. Multiple factors involved in the preparation of the engineered immunosensor, including: high rate electron transfer capability that confirms excellent electrical conductivity of desired matrix, structural properties and high stability of the Cys-GA interface, extensive and appropriate surface area, the optimal reaction of designed interface with biological components for antibody immobilization, and providing the possibility of biological activity. All mentioned parameters can be considered as the results which is provide an appropriate sensitivity of biosensors.

3.3.2. *Sensitivity study of engineered immunosensor in human saliva sample*

According to Fig. 8A, SWVs was recorded for the evaluation of engineered immunosensor capability to detection of various concentration of Cyfra21.1 biomarker in human saliva sample. For this purpose, SWVs were performed in the potential range of -1 to +1 V and sweep rate of 100 mV/s in different concentrations of Cyfra21.1 biomarker and the ability of the technique was evaluated to measurements of the Cyfra21.1 biomarker in human plasma sample.

As well as in Fig. 8B, the calibration curve of proposed immunosensor for 2.5–50 ng/ml concentration of Cyfra21.1 in human saliva samples was plotted and the following linear regression equation was obtained:

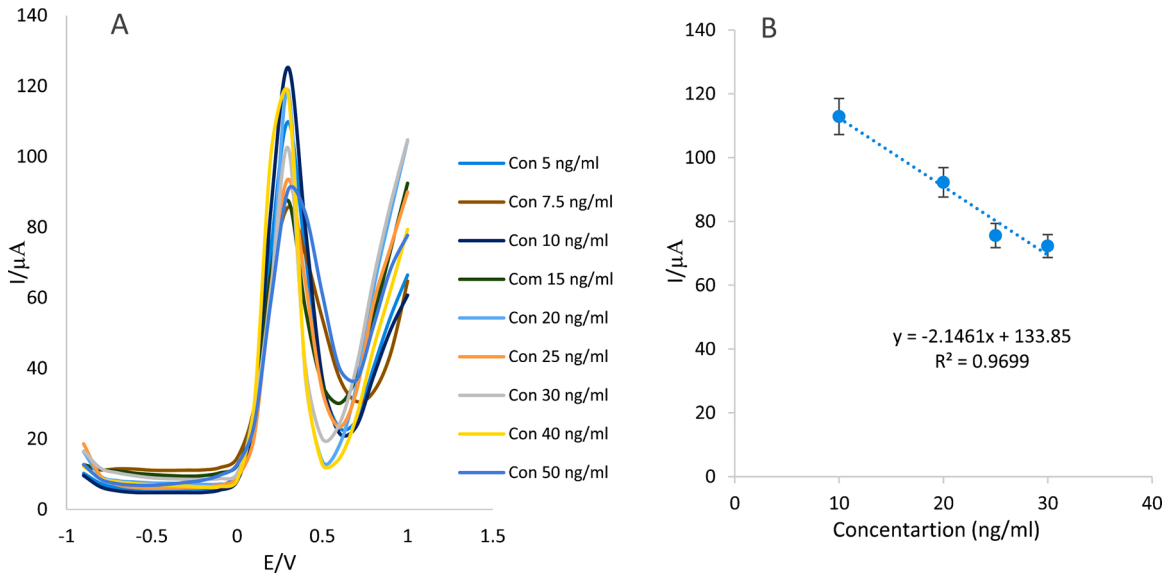

Fig. 9. A) SWVs responses of the immunosensor for different diluted concentrations of Cyfra21.1: 5, 7.5, 10, 15, 20, 25, 30, 40, and 50 ng/mL in human saliva sample in 0.01 M [Fe (CN)6]3-/4- solution containing KCl B) Calibration curve (n = 5, Sd = 2.10, Sd = 1.98, Sd = 1.97, and Sd = 1.98, for concentrations of 10, 20, 25, and 30 ng/mL, respectively)).

$I\ (\mu A) = -0.6458\ C_{(Cyfra21.1)} + 95.293,\ R^2 = 0.9566.$

The LLOQ for the detection of Cyfra21.1 antigen in human saliva sample was recorded as 2.5 ng /mL. as proposed, different concentrations of the Cyfra21.1 antigen between 5 ng/mL to 50 ng/mL were prepared. Diluted concentrations were 5, 7, 10, 15, 20, 25, 30, 40, 50 ng/mL. According to Fig. 9A, the evaluation was performed in the range of 5 ng/mL to 50 ng/mL by mentioned diluting concentrations of biomarker in human saliva sample using SWV technique.

The linear regressions equation obtained as follows:

$I\ (\mu A) = -2.1461C_{(Cyfra21.1)} + 133.85,\ R^2 = 0.9699.$

Several studies have been performed on the measurement of Cyfra21.1 biomarkers in various biological samples using conventional non-biosensing methods to diagnose OC. In the following, we survey the results of this research.

In 1997, Kurokawa and coworkers [61] measured serum level of Cyfra 21.1 in relation to oral cancer by immunoradiometric assay and reported a significant concentration in patients with oral cancer higher than the control population (n = 42, 2.25 ng.ml^{-1}).

Kawaguchi et al., [62] measured the Cyfra 21.1 in serum sample using the immunoassay radiometric assay method and reported its concentration as 2.9 ng.ml^{-1}. Also, Zhong et al., [39,63] studied both salivary and serum samples using the enzyme-linked immunosorbent assay (ELISA) method for Cyfra 21.1 detection. The serum sample showed a concentration of 0.65 µg/L and sensitivity and specificity of 0.570 and 0.964, respectively. In the salivary sample study, the measured concentration was reported at 85.95 µg/L and the sensitivity and specificity of 0.5 and 0.86, respectively.

Interestingly, Rajkumar and colleagues [36] conducted a comparative study between the serum and salivary levels of the Cyfra21.1 biomarker by ELISA, which measured serum levels in patients at 5.14 ng.ml^{-1} and salivary levels at 17.46 ng.ml^{-1}. Also, Malhotra and colleagues [64] reported a concentration of 13.68 ng.ml^{-1} and 5.01 ng.ml^{-1} in 2016, using the electrochemiluminescence (ECL) immunoassay (ECLIA) method in the analysis of salivary and serum samples, respectively.

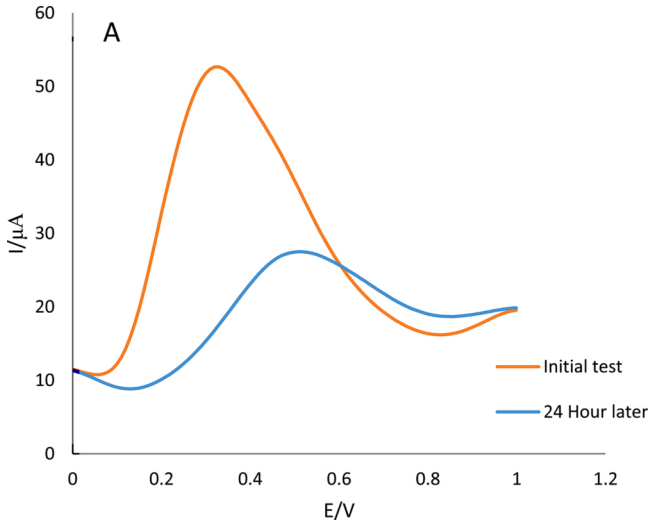

Fig. 10. A) SWVs and B) histograms for the stability study of CysA-GA/AuE in potential range of -1 to +1 and sweep 100 mV/s in 0.01 M [Fe (CN) 6]3-/4- solution containing KCl at 24 -h intervals. ([n = 5, Sd; 2.06] and [n = 3 Sd = 1.18] for initial test and 24 h, resepcticely).

Table 1
A comparison of the performance of several assay strategies for the detection of Cyfra21.1.

Assay strategies	Platform	Technique	Sample	LOD/ LLOQ	Linear range	Ref
Immunosensor	APTES/nHfo$_2$/ITO	CV	saliva	0.21 ng/mL	2–18 ng/mL	[65]
Immunosensor	APTES-Zro$_2$ /ITO	CV	saliva	0.08 ng/mL	2–16 ng/mL	[66]
Immunosensor	APTES/Zro$_2$ RGO/ITO	DPV	saliva	0.122 ng/mL	2–22 ng/mL	[67]
Immunosensor	Cys-La(OH)$_3$/ITO	DPV	saliva	0.001 ng/mL	0.001–10.2 ng/mL	[68]
Immunosensor	CysA-GA/AuE	SWV	saliva	2.5 ng/mL	2.5–50 ng/mL	This work

LOD; Limit of detection, **LLOQ**; Low limit of quantification, **CV;** Cyclic voltammetry, **DPV**; Differential pulse voltammetry, SWV; Square wave voltammetry.

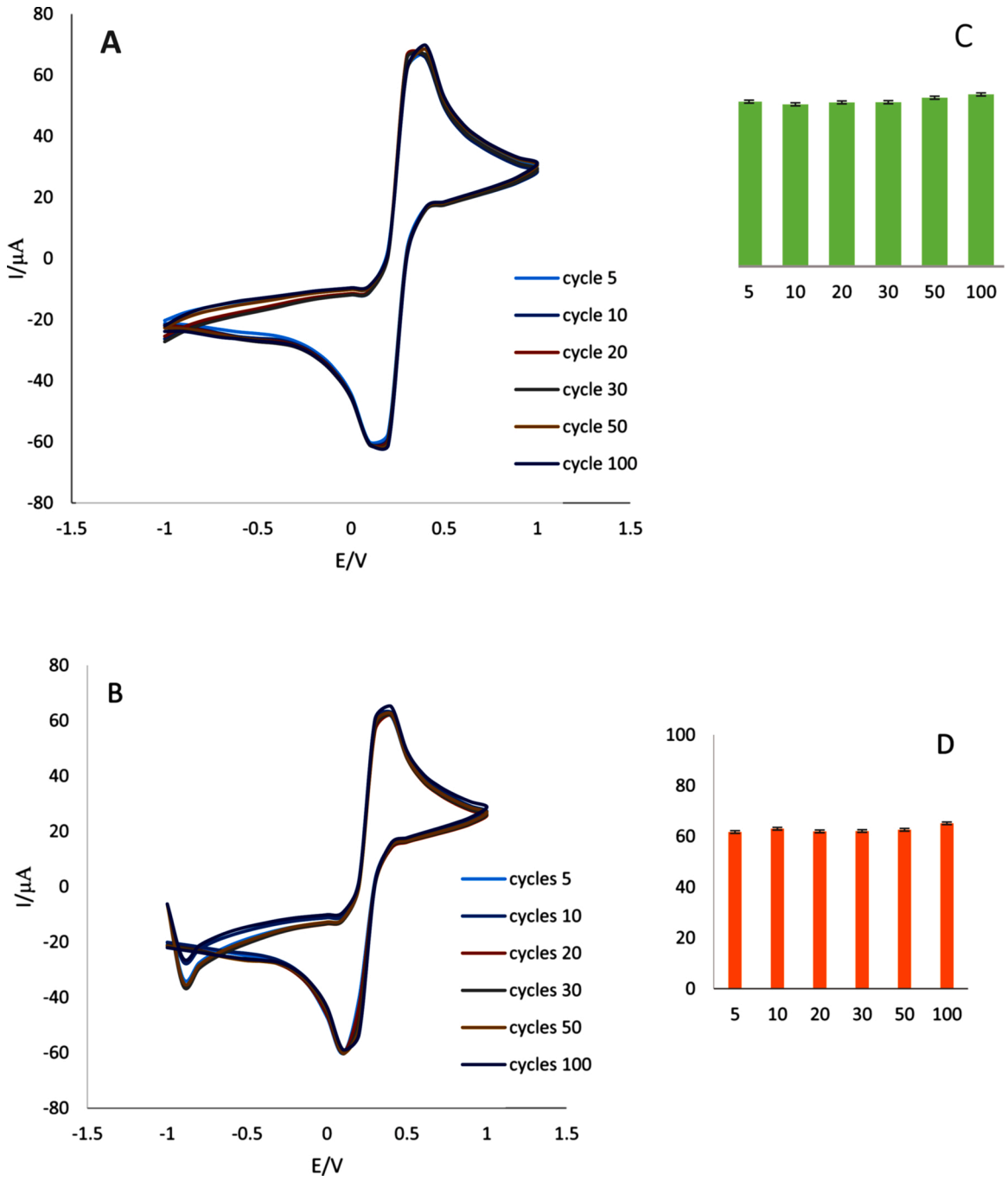

Fig. 11. Cyclic voltammograms of CysA/AuE (A) and CysA-GA/AuE (B) stability study in potential range of -1 to +1 and sweep rate of 100 mV/s Number of cycles were 5, 10, 20, 30, 50 cycles in 0.01 M [Fe (CN) 6]3-/4- solution containing KCl. C and D) related histograms.

In addition, the results of several studies to evaluate Cyfra 21.1 biomarkers for OC detection in the salivary sample using the immunosensing method are compared with the results of the current research in Table 1.

3.4. Stability study

3.4.1. Investigating the stability of engineered immunosensor in the daily intervals times

The stability assessment of the CysA-GA-anti-Cyfra21.1 antibody-BSA-Cyfra21.1 antigen/AuE immunosensor was performed by SWVs technique in the potential range of -1 to +1 V and sweep rate of 100 mV /s in 0.01 M [Fe (CN) $_6$] $^{-3/-4}$ solutions and in 24 -h intervals. The immunosensor susceptibility to reuse is important in real-time applications such as clinical diagnosis which depends on the stability and the ability to reconstruct immunosensor. For this purpose, immunosensor was stored at 4 °C for 24 h. Then, SWV were recorded in two stage (immediately after preparation of bio-device and after 24 h). The results obtained from SWVs (Fig. 10) reveal that the CysA-GA-anti-Cyfra21.1 antibody-BSA-Cyfra21.1 antigen/AuE immunosensor shows acceptable stability within 24 h.

3.4.2. Cyclic stability study of engineered interface

The stability of CysA and CysA-GA interfaces was investigated by CVs technique based on the number of cycles and the results were revealed in Fig. 11A and B respectively. To evaluation of both matrix stability, CVs

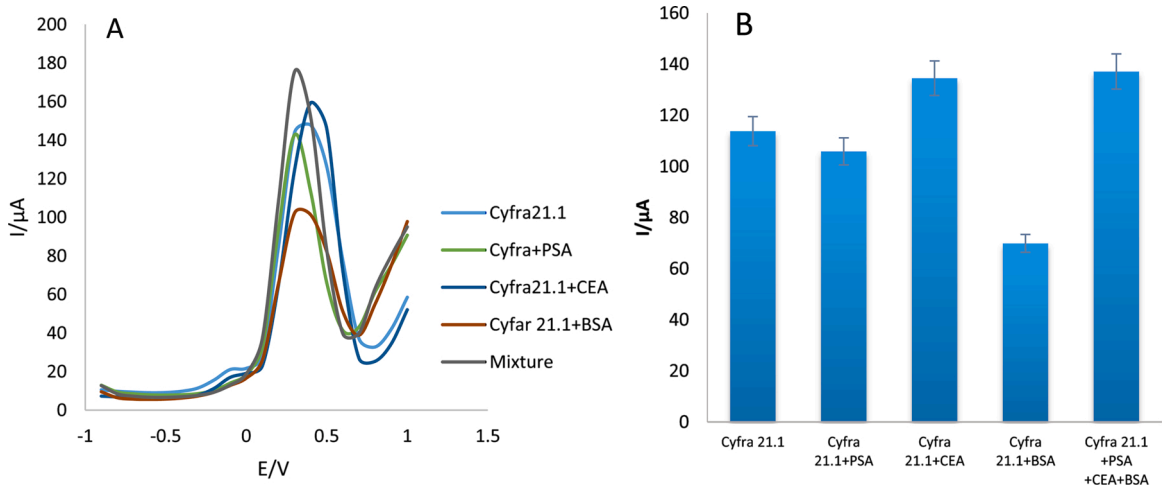

Fig. 12. A) SWVs of CysA-GA-anti-Cyfra21.1-BSA-Cyfra21.1 antigen/AuE immunosensor in the presence of BSA, PSA, CEA and mixture (BSA, PSA, CEA, Cyfra21.1) as interferer. B) Related histograms. All evaluation carried on 0.01 M [Fe (CN) 6]3-/4- solution containing KCl in potential range of -1 to +1 V. ([n = 3, Sd = 1.90], [n = 3, Sd = 1.71], [n = 3, Sd = 1.80], [n = 3, and Sd = 1.4], and [n = 3, Sd = 1.80], for (Cyfra21.1), (Cyfra21.1 + PSA), (Cyfra21.1 + CEA), (Cyfra21.1 + BSA, and (Cyfra21.1 + PSA + CEA + BSA), respectively).

performed in 5, 10, 20, 30, 50 and 100 cycles in in 0.01 M $[Fe(CN)_6]^{-3/-4}$ as mediator solution. According to the obtained results, it is observed that Cys/AuE and Cys-GA/AuE matrices, which are prepared via self-assembly, are completely stable. CVs reveals that increasing the number of cycles, there is no change in the peak's current.

3.5. Selectivity of engineered immunosensor

To evaluate the selectivity of the engineered immunosensor, for the precise and accurate determination of Cyfra 21.1 biomarker, a number of biomolecules interferers such as PSA, BSA and CEA which can be interfere on the performance of bio-device and their mixtures were investigated by SWVs techniques.

As results are shown in SWVs voltammogram for CAE, BSA, PSA and their mixture (Fig. 12), the peak's currents obtained from Cyfra21.1 were compared with interferer species. The results demonstrate that PSA has no interfere in Cyfra21.1 detection, although, CEA increasing intensity of Cyfra21.1 peak's currents and BSA decrease it. The results confirm that CEA and BSA are interfere in Cyfra21.1 detection. Also, the mixture of selected biomolecules lead to increase of Cyfra21.1 peak's current that reveals CEA as dominant interfere.

3.6. Reproducibility, precision, stability and regeneration of the immunosensor

The reproducibility of the immunosensor was evaluated assessed by fabricating five modified electrodes independently at under the same experimental condition, and using them for detection of 5–50 ng/L of Cyfra21.1. The relative standard deviations were 1.42 % and 1.79 % for detection of 5–50 ng/L of Cyfra21.1, respectively. These results suggested the acceptable satisfactory fabrication reproducibility and precision of the immunosensor. The long time long-time stability of the immunosensor was also investigated by storing it in at 4 °C in refrigerator. The response of the immunosensor for 50 ng/L of Cyfra21.1 after 10 days was about 97 % of its initial response. For 5 ng/L of Cyfra21.1, the same stability was observed and after one week the immunosensor response was about 95.1 % of its initial response. Regeneration is a key factor for developing a practical immunosensor. After the immunosensor was used to detect Cyfra21.1, the modified electrode was treated with 3 M of urea solution for 30 min to dissociate detach the antigen-antibody linkage. After rinsing with distilled water, we used the regenerated immunosensors were used to detect the same Cyfra21.1 concentration. The RSD of 1.54 % was obtained for four regenerated immunosensors at in the Cyfra21.1 concentration of 50 ng/L. The effect of Cyfra21.1concentration on reproducibility of the system was also investigated. In the presence of 5–50 ng/L of Cyfra21.1for four regenerated immunosensors, the RSD were 1.99 % and 2.31 %, respectively. This result indicates indicated that the antibody has the same activity at in a wide concentration range of Cyfra21.1.

4. Conclusion

In this research, an innovative immunosensor (Cys-GA-anti-Cyfra21.1 antibody-BSA-Cyfra21.1 antigen/AuE) was successfully designed and developed to the detection and determination of the Cyfra21.1 biomarker in unprocessed human saliva sample towards early diagnosis of OC. The Au electrode was modified by Cys and GA respectively via self-assembly as a substrate to immobilize the biological agents. The engineered immunosensor exhibit the excellent ability to detect and determine of Cyfra21.1 biomarker in low concentrations of the desired biomarker in unprocessed human saliva sample. Under the optimized operating conditions, the results demonstrate that the desired platform has a good sensitivity detection of Cyfra21.1 with the low limit of quantitation (LLOQ) of 2.5 ng/mL, which this evaluation was performed at a wide linear range of 2.5−50 ng/mL.

The use of the CysA-GA nano-hybrid as extraordinary stable substrate and extensive platform to place recognition elements was investigated using various electrochemical methods including CV, SWV. In this study, the engineered biosensor was used to non-invasive detection of Cyfra21.1 in unprocessed human saliva sample without the need to extra treatments. Based on the obtained results, CysA-GA-anti-Cyfra21.1-BSA-Cyfra21.1 antigen/AuE immunosensor with significantly high current intensity can provide appropriate, reliable, affordable, quick, and user-friendly diagnostic device to monitoring oral abnormality by detection and determination of Cyfra21.1 biomarker in human real sample. Given the increasing importance of prevention, prognosis, and early-stage diagnosis of cancer in improving of survival rate, the use of diagnostic devices is essential. Above all, the easy to prepared designed immunosensor can be an extremely promising candidate to specific and favorable for a vast range of electrochemical immunosensing applications.

Declaration of Competing Interest

The authors report no declarations of interest.

Acknowledgement

This work was supported by TBZMED (Tabriz University of Medical Sciences)-Grant Number 59915- IR.TBZMED.VCR.REC.1397.031.

References

[1] K. Dhanuthai, S. Rojanawatsirivej, W. Thosaporn, S. Kintarak, A. Subarnbhesaj, M. Darling, E. Kryshtalskyj, C.P. Chiang, H.I. Shin, S.Y. Choi, S.S. Lee, P. Aminishakib, Oral cancer: a multicenter study, Med. Oral Patol. Oral Cir. Bucal 23 (1) (2018) e23–e29.
[2] V. Vucicevic Boras, A. Fucic, M. Virag, D. Gabric, I. Blivajs, C. Tomasovic-Loncaric, Z. Rakusic, V. Bisof, N.L. Novere, D. Velimir Vrdoljak, Significance of stroma in biology of oral squamous cell carcinoma, Tumori 104 (1) (2018) 9–14.
[3] S.A. Liu, W.C. Tsai, Y.K. Wong, J.C. Lin, C.K. Poon, S.Y. Chao, Y.L. Hsiao, M. Y. Chan, C.S. Cheng, C.C. Wang, Nutritional factors and survival of patients with oral cancer, Head Neck 28 (11) (2006) 998–1007.
[4] B.M. Robert, M. Dakshinamoorthy, B. Ganapathyagraharam Ramamoorthy, M. Dhandapani, R. Thangaiyan, G. Muthusamy, R.M. Nirmal, N.R. Prasad, Predicting tumor sensitivity to chemotherapeutic drugs in oral squamous cell carcinoma patients, Sci. Rep. 8 (1) (2018) 15545.
[5] F.R. Pires, A.B. Ramos, J.B.Cd. Oliveira, A.S. Tavares, P.S.Rd. Luz, T.C.R. Bd. Santos, Oral squamous cell carcinoma: clinicopathological features from 346 cases from a single oral pathology service during an 8-year period, J. Appl. Oral Sci. 21 (5) (2013) 460–467.
[6] P. Sharma, S. Saxena, P. Aggarwal, Trends in the epidemiology of oral squamous cell carcinoma in Western UP: an institutional study, Indian J. Dent. Res. 21 (3) (2010) 316–319.
[7] J. Ferlay, I. Soerjomataram, R. Dikshit, S. Eser, C. Mathers, M. Rebelo, D.M. Parkin, D. Forman, F. Bray, Cancer incidence and mortality worldwide: sources, methods and major patterns in GLOBOCAN 2012, Int. J. Cancer 136 (5) (2015) E359–E386.
[8] K.D. Shield, J. Ferlay, A. Jemal, R. Sankaranarayanan, A.K. Chaturvedi, F. Bray, I. Soerjomataram, The global incidence of lip, oral cavity, and pharyngeal cancers by subsite in 2012, CA Cancer J. Clin. 67 (1) (2017) 51–64.
[9] S. Warnakulasuriya, Global epidemiology of oral and oropharyngeal cancer, Oral Oncol. 45 (4-5) (2009) 309–316.
[10] A.J. Tuyns, J. Estève, L. Raymond, F. Berrino, E. Benhamou, F. Blanchet, P. Boffetta, P. Crosignani, A. del Moral, W. Lehmann, et al., Cancer of the larynx/hypopharynx, tobacco and alcohol: IARC international case-control study in Turin and Varese (Italy), Zaragoza and Navarra (Spain), Geneva (Switzerland) and Calvados (France), Int. J. Cancer 41 (4) (1988) 483–491.
[11] S. Petti, Lifestyle risk factors for oral cancer, Oral Oncol. 45 (4-5) (2009) 340–350.
[12] I. Khan, N. Kumar, I. Pant, S. Narra, P. Kondaiah, Activation of TGF-β pathway by areca nut constituents: a possible cause of oral submucous fibrosis, PLoS One 7 (12) (2012), e51806.
[13] V. Jayaprakash, M. Reid, E. Hatton, M. Merzianu, N. Rigual, J. Marshall, S. Gill, J. Frustino, G. Wilding, T. Loree, S. Popat, M. Sullivan, Human papillomavirus types 16 and 18 in epithelial dysplasia of oral cavity and oropharynx: a meta-analysis, 1985-2010, Oral Oncol. 47 (11) (2011) 1048–1054.
[14] K. Gupta, R. Metgud, Evidences suggesting involvement of viruses in oral squamous cell carcinoma, Patholog. Res. Int. 2013 (2013), 642496.
[15] Y. She, X. Nong, M. Zhang, M. Wang, Epstein-Barr virus infection and oral squamous cell carcinoma risk: a meta-analysis, PLoS One 12 (10) (2017) e0186860.
[16] D.F. Gualtero, A. Suarez Castillo, Biomarkers in saliva for the detection of oral squamous cell carcinoma and their potential use for early diagnosis: a systematic review, Acta Odontol. Scand. 74 (3) (2016) 170–177.
[17] J. Noguti, C.F. De Moura, G.P. De Jesus, V.H. Da Silva, T.A. Hossaka, C.T. Oshima, D.A. Ribeiro, Metastasis from oral cancer: an overview, Cancer Genomics Proteomics 9 (5) (2012) 329–335.
[18] S. Irani, Distant metastasis from oral cancer: a review and molecular biologic aspects, J. Int. Soc. Prev. Commun. Dent. 6 (4) (2016) 265–271.
[19] Q. Wang, P. Gao, X. Wang, Y. Duan, The early diagnosis and monitoring of squamous cell carcinoma via saliva metabolomics, Sci. Rep. 4 (1) (2014) 6802.
[20] Q. Wang, P. Gao, X. Wang, Y. Duan, Investigation and identification of potential biomarkers in human saliva for the early diagnosis of oral squamous cell carcinoma, Clin. Chim. Acta 427 (2014) 79–85.
[21] M. Jafari, M. Hasanzadeh, Cell-specific frequency as a new hallmark to early detection of cancer and efficient therapy: recording of cancer voice as a new horizon, Biomed. Pharmacother. 122 (2020), 109770.
[22] R. Mishra, Biomarkers of oral premalignant epithelial lesions for clinical application, Oral Oncol. 48 (7) (2012) 578–584.
[23] P. Güneri, J.B. Epstein, Late stage diagnosis of oral cancer: components and possible solutions, Oral Oncol. 50 (12) (2014) 1131–1136.
[24] R. Mehrotra, D.K. Gupta, Exciting new advances in oral cancer diagnosis: avenues to early detection, Head Neck Oncol. 3 (2011) 33.
[25] Z.S. Peacock, M.A. Pogrel, B.L. Schmidt, Exploring the reasons for delay in treatment of oral cancer, J. Am. Dent. Assoc. 139 (10) (2008) 1346–1352.
[26] S. Fedele, Diagnostic aids in the screening of oral cancer, Head Neck Oncol. 1 (1) (2009) 1–6.
[27] M. Hasanzadeh, N. Shadjou, M. de la Guardia, Non-invasive diagnosis of oral cancer: the role of electro-analytical methods and nanomaterials, TrAC Trends Anal. Chem. 91 (2017) 125–137.
[28] M. Hasanzadeh, E. Solhi, M. Jafari, A. Mokhtarzadeh, J. Soleymani, A. Jouyban, S. Mahboob, Ultrasensitive immunoassay of tumor protein CA 15.3 in MCF-7 breast cancer cell lysates and unprocessed human plasma using gold nanoparticles doped on the structure of mesoporous silica, Int. J. Biol. Macromol. 120 (2018) 2493–2508.
[29] M. Jafari, E. Solhi, S. Tagi, M. Hasanzadeh, V. Jouyban-Gharamaleki, A. Jouyban, N. Shadjou, Non-invasive quantification of malondialdehyde biomarker in human exhaled breath condensate using self-assembled organic-inorganic nanohybrid: a new platform for early diagnosis of lung disease, J. Pharm. Biomed. Anal. 164 (2019) 249–257.
[30] M. Jafari, M. Hasanzadeh, E. Solhi, S. Hassanpour, N. Shadjou, A. Mokhtarzadeh, A. Jouyban, S. Mahboob, Ultrasensitive bioassay of epitope of Mucin-16 protein (CA 125) in human plasma samples using a novel immunoassay based on silver conductive nano-ink: a new platform in early stage diagnosis of ovarian cancer and efficient management, Int. J. Biol. Macromol. 126 (2019) 1255–1265.
[31] T. Radhika, N. Jeddy, S. Nithya, R.M. Muthumeenakshi, Salivary biomarkers in oral squamous cell carcinoma - an insight, J. Oral Biol. Craniofac. Res. 6 (Suppl. 1) (2016) S51–S54.
[32] A. Eftekhari, M. Hasanzadeh, S. Sharifi, S.M. Dizaj, R. Khalilov, E. Ahmadian, Bioassay of saliva proteins: the best alternative for conventional methods in non-invasive diagnosis of cancer, Int. J. Biol. Macromol. 124 (2019) 1246–1255.
[33] A.K. Markopoulos, E.Z. Michailidou, G. Tzimagiorgis, Salivary markers for oral cancer detection, Open Dent. J. 4 (2010) 172–178.
[34] H. Xiao, L. Zhang, H. Zhou, J.M. Lee, E.B. Garon, D.T. Wong, Proteomic analysis of human saliva from lung cancer patients using two-dimensional difference gel electrophoresis and mass spectrometry, Mol. Cell Proteomics 11 (2) (2012). M111.012112.
[35] L.R. Bigler, C.F. Streckfus, W.P. Dubinsky, Salivary biomarkers for the detection of malignant tumors that are remote from the oral cavity, Clin. Lab. Med. 29 (1) (2009) 71–85.
[36] K. Rajkumar, R. Ramya, G. Nandhini, P. Rajashree, A. Ramesh Kumar, S. Nirmala Anandan, Salivary and serum level of CYFRA 21-1 in oral precancer and oral squamous cell carcinoma, Oral Dis. 21 (1) (2015) 90–96.
[37] R. Mishra, Cell cycle-regulatory cyclins and their deregulation in oral cancer, Oral Oncol. 49 (6) (2013) 475–481.
[38] Q. Li, X. Ouyang, J. Chen, P. Zhang, Y. Feng, A review on salivary proteomics for oral Cancer screening, Curr. Issues Mol. Biol. 37 (2020) 47–56.
[39] L.-p. Zhong, C.-p. Zhang, J.-w. Zheng, J. Li, W.-t. Chen, Z.-y. Zhang, Increased Cyfra 21-1 concentration in saliva from primary oral squamous cell carcinoma patients, Arch. Oral Biol. 52 (11) (2007) 1079–1087.
[40] Y.X. Wang, D. Hu, X. Yan, Diagnostic accuracy of Cyfra 21-1 for head and neck squamous cell carcinoma: a meta-analysis, Eur. Rev. Med. Pharmacol. Sci. 17 (17) (2013) 2383–2389.
[41] P. Singh, S.R. Barpande, J.D. Bhavthankar, M.S. Mandale, A.U. Bhagwat, Serum Cyfra 21-1 levels in oral squamous cell carcinoma patients and its clinicopathologic correlation, Indian J. Dent. Res. 28 (2) (2017) 162–168.
[42] A.M. AlAli, T. Walsh, M. Maranzano, CYFRA 21-1 and MMP-9 as salivary biomarkers for the detection of oral squamous cell carcinoma: a systematic review of diagnostic test accuracy, Int. J. Oral Maxillofac. Surg. (2020).
[43] R. Malhotra, A. Urs, A. Chakravarti, S. Kumar, V. Gupta, B. Mahajan, Correlation of Cyfra 21-1 levels in saliva and serum with CK19 mRNA expression in oral squamous cell carcinoma, Tumor Biol. 37 (2016).
[44] M. Hasanzadeh, N. Shadjou, Electrochemical and photoelectrochemical nano-immunesensing using origami paper based method, Mater. Sci. Eng. C 61 (2016) 979–1001.
[45] T.R.J. Holford, F. Davis, S.P.J. Higson, Recent trends in antibody based sensors, Biosens. Bioelectron. 34 (1) (2012) 12–24.
[46] M. Yang, A. Javadi, S. Gong, Sensitive electrochemical immunosensor for the detection of cancer biomarker using quantum dot functionalized graphene sheets as labels, Sens. Actuators B Chem. 155 (1) (2011) 357–360.
[47] F. Farshchi, M. Hasanzadeh, E. Solhi, Immunosensing of prostate cancer in human plasma samples using immobilization of antibody on the surface of mesoporous silica-modified silver nanoparticles and its immunocomplex with prostate-specific antigen, Anal. Methods 11 (48) (2019) 6159–6167.
[48] M. Hasanzadeh, A. Mohammadzadeh, M. Jafari, B. Habibi, Ultrasensitive immunoassay of glycoprotein 125 (CA 125) in untreated human plasma samples using poly (CTAB-chitosan) doped with silver nanoparticles, Int. J. Biol. Macromol. 120 (Pt B) (2018) 2048–2064.
[49] M. Hasanzadeh, N. Shadjou, M. de la Guardia, Electrochemical biosensing using hydrogel nanoparticles, TrAC Trends Anal. Chem. 62 (2014) 11–19.
[50] M. Hasanzadeh, N. Shadjou, Electrochemical nanobiosensing in whole blood: recent advances, TrAC Trends Anal. Chem. 80 (2016) 167–176.
[51] M. Moradkhani, F. Farshchi, M. Hasanzadeh, A. Mokhtarzadeh, A novel bioassay for the monitoring of carcinoembryonic antigen in human biofluid using polymeric interface and immunosensing method, J. Mol. Recognit. (2020) e2852, n/a(n/a).
[52] A. Mokhtarzadeh, R. Eivazzadeh-Keihan, P. Pashazadeh, M. Hejazi, N. Gharaatifar, M. Hasanzadeh, B. Baradaran, M. de la Guardia, Nanomaterial-based biosensors for detection of pathogenic virus, TrAC Trends Anal. Chem. 97 (2017) 445–457.
[53] B. Wang, U. Akiba, J.I. Anzai, Recent progress in nanomaterial-based electrochemical biosensors for cancer biomarkers: a review, Molecules 22 (7) (2017).
[54] M. Hasanzadeh, S. Tagi, E. Solhi, A. Mokhtarzadeh, N. Shadjou, A. Eftekhari, S. Mahboob, An innovative immunosensor for ultrasensitive detection of breast cancer specific carbohydrate (CA 15-3) in unprocessed human plasma and MCF-7 breast cancer cell lysates using gold nanospear electrochemically assembled onto thiolated graphene quantum dots, Int. J. Biol. Macromol. 114 (2018) 1008–1017.

[55] Q. Cai, B. Xu, L. Ye, Z. Di, J. Zhang, Q. Jin, J. Zhao, J. Xue, X. Chen, Immobilization of biomolecules on cysteamine-modified polyaniline film for highly sensitive biosensing, Talanta 120 (2014) 462–469.
[56] D. Du, W. Chen, J. Cai, J. Zhang, F. Qu, H. Li, Development of acetylcholinesterase biosensor based on CdTe quantum dots modified cysteamine self-assembled monolayers, J. Electroanal. Chem. (Lausanne) 623 (1) (2008) 81–85.
[57] M.Ç. Canbaz, Ç.S. Şimşek, M.K. Sezgintürk, Electrochemical biosensor based on self-assembled monolayers modified with gold nanoparticles for detection of HER-3, Anal. Chim. Acta 814 (2014) 31–38.
[58] D.K. Schwartz, Mechanisms and kinetics of self-assembled monolayer formation, Annu. Rev. Phys. Chem. 52 (1) (2001) 107–137.
[59] C.S. Park, R. Colorado, A.C. Jamison, T.R. Lee, Thiol-Based Self-Assembled Monolayers: Formation, Organization, and the Role of Adsorbate Structure, 2016.
[60] N.K. Chaki, K. Vijayamohanan, Self-assembled monolayers as a tunable platform for biosensor applications, Biosens. Bioelectron. 17 (1) (2002) 1–12.
[61] H. Kurokawa, Y. Yamashita, S. Tokudome, M. Kajiyama, Combination assay for tumor markers in oral squamous cell carcinoma, J. Oral Maxillofac. Surg. 55 (9) (1997) 964–966.
[62] H. Kawaguchi, S. Ohno, M. Miyazaki, K. Hashimoto, A. Egashira, H. Saeki, M. Watanabe, K. Sugimachi, CYFRA 21-1 determination in patients with esophageal squamous cell carcinoma: clinical utility for detection of recurrences, Cancer 89 (7) (2000) 1413–1417.
[63] L.P. Zhong, H.G. Zhu, C.P. Zhang, W.T. Chen, Z.Y. Zhang, Detection of serum Cyfra 21-1 in patients with primary oral squamous cell carcinoma, Int. J. Oral Maxillofac. Surg. 36 (3) (2007) 230–234.
[64] R. Malhotra, A.B. Urs, A. Chakravarti, S. Kumar, V.K. Gupta, B. Mahajan, Correlation of Cyfra 21-1 levels in saliva and serum with CK19 mRNA expression in oral squamous cell carcinoma, Tumor Biol. 37 (7) (2016) 9263–9271.
[65] S. Kumar, S. Kumar, S. Tiwari, S. Augustine, S. Srivastava, B.K. Yadav, B. D. Malhotra, Highly sensitive protein functionalized nanostructured hafnium oxide based biosensing platform for non-invasive oral cancer detection, Sens. Actuators B Chem. 235 (2016) 1–10.
[66] S. Kumar, S. Kumar, S. Tiwari, S. Srivastava, M. Srivastava, B.K. Yadav, S. Kumar, T.T. Tran, A.K. Dewan, A. Mulchandani, J.G. Sharma, S. Maji, B.D. Malhotra, Biofunctionalized nanostructured zirconia for biomedical application: a smart approach for oral cancer detection, Adv. Sci. 2 (8) (2015), 1500048.
[67] S. Kumar, J.G. Sharma, S. Maji, B.D. Malhotra, Nanostructured zirconia decorated reduced graphene oxide based efficient biosensing platform for non-invasive oral cancer detection, Biosens. Bioelectron. 78 (2016) 497–504.
[68] S. Tiwari, P.K. Gupta, Y. Bagbi, T. Sarkar, P.R. Solanki, L-cysteine capped lanthanum hydroxide nanostructures for non-invasive detection of oral cancer biomarker, Biosens. Bioelectron. 89 (2017) 1042–1052.